Maleic Anhydride Crosslinked Alginate-Chitosan Blend Membranes for Pervaporation of Ethylene Glycol-Water Mixtures

Alla Subba Reddy[a]; Nadavala Siva Kumar[a]; Munagapati Venkata Subbaiah[a]; Madala Suguna[a]; Abburi Krishnaiah[a]

[a] Biopolymers and Thermophysical Laboratory, Department of Chemistry, Sri Venkateswara University, Tirupati, India

PLEASE SCROLL DOWN FOR ARTICLE

Maleic Anhydride Crosslinked Alginate-Chitosan Blend Membranes for Pervaporation of Ethylene Glycol-Water Mixtures

ALLA SUBBA REDDY, NADAVALA SIVA KUMAR, MUNAGAPATI VENKATA SUBBAIAH,
MADALA SUGUNA and ABBURI KRISHNAIAH*

*Biopolymers and Thermophysical Laboratory, Department of Chemistry, Sri Venkateswara University,
Tirupati, India*

Calcium alginate-chitosan (CA/CS) blended membranes were prepared and crosslinked with maleic anhydride (MA) for the pervaporation (PV) separation of ethylene glycol (EG)/water mixtures at 30°C. The structure and properties of blend membranes were studied with the aid of FTIR, XRD, TGA, and SEM. The effect of experimental parameters such as feed composition, membrane thickness, and permeate pressure on separation performance of the MA crosslinked membranes were determined in terms of flux, selectivity, and pervaporation separation index. Sorption studies were carried out to evaluate the extent of interaction and degree of swelling of the blend membranes in pure, as well as in binary mixtures. The experimental results suggested that the crosslinked membrane (M-CA/CS) exhibited a good selectivity of 302 at a normalized flux of 0.38 kg.m^{-2}.h^{-1}.10 μm at 30°C for 96.88 wt% EG aqueous solution.

Keywords: Pervaporation, calcium alginate, chitosan, ethylene glycol, maleic anhydride

1 Introduction

Ethylene glycol (EG) is an important chemical widely used as a starting material in the polyester industry, antifreezing agent in automobile cooling systems and many other industrial products (1). At present, EG is commercially produced by direct oxidation of ethylene to ethylene oxide followed by hydrolysis of ethylene oxide. During this process, excess water is added to ethylene oxide in order to increase EG yield. Although EG and water do not form an azeotrope over the entire composition range, the removal of water from EG by multi-stage distillation has proven to be energy intensive process due to high boiling point of EG (197°C) (2). In fact, EG-water separation by distillation is ranked as the eighth most energy intensive distillation operation in the chemical process industry (3). In comparison, PV will become a feasible and promising alternative, because it could run at a relative low temperature and requires less energy (4, 5).

The membrane based pervaporation (PV) technique has been industrialized in many countries over the past decade (6). It has many advantages such as high separation efficiency, low energy consumption, simple operation, environmental benign (7), in addition, it offers an opportunity for the separation of organic liquid mixtures and organic contaminated industrial wastewater besides being safe for handling heat-sensitive and hazardous compounds (8, 9). Furthermore, it is suitable for the separation of azeotropic and close boiling mixtures, because the separation mechanism in PV is not based on relative volatility of the components, but on the difference in sorption and diffusion properties of feed components as well as permselectivity of the membrane (10, 11). In the pervaporation process, the membrane material is a key factor for separation efficiency. It is a well-known fact that ionomer membranes possess high affinity for water molecules due to the presence of ionic sites in such polymers (9, 12).

Sodium alginate (SA) and chitosan (CS), the natural anionic and cationic polysaccharides respectively, have been used extensively to synthesize membranes for PV separation studies due to their abundant availability, biocompatibility, biodegradability, and commercial viability (9). SA is highly soluble in water and available in marine algae and seaweeds. It has good membrane forming properties with other polymers in addition to good chemical resistance and high permselectivity to water. However, very high hydrophilicity of carboxylic and hydroxyl groups present in

*Address correspondence to: A. Krishnaiah, Department of Chemistry, S.V. University, Tirupati-517502, India. Tel.: +91-9393621986; E-mail: abburikrishnaiah@gmail.com

SA renders the membrane unstable in aqueous solution during PV. Water solubility and mechanical weakness of alginic acid membrane has been a drawback in its possible use as a pervaporation material in spite of its excellent permselectivity for water. To improve the mechanical stability of membrane, SA needs to be blended with other polymer. In the past few years, CS was found to be very attractive material for the preparation of hydrophilic membranes. CS is deacetylated form of chitin (13, 14), which is available in abundance in the crustacean shells such as crab and shrimp. CS has been proven to have good film forming properties with mechanical, chemical resistance and high permselectivity for water. CS has both reactive amino and hydroxyl groups that can participate in chemical reactions such as salt formation (15). These hydrophilic groups are considered to play an important role in preferential water sorption and diffusion through the CS membrane.

Till now, several kinds of polymer-based materials have been employed in the dehydration process of EG aqueous solution by PV, e.g. chitosan (16–18), poly(vinyl alcohol) (PVA) (19–25), interpenetrating polymer network (IPN) membranes (26), sulfonated polyethylene (27), several GFT (plasma polymerized and PVA/PAN) composite membranes (28), sulfonated poly(ether ether ketone) (29, 30) and poly(*N*, *N*-dimethylaminoethyl methacrylate) (31). In the present investigation, membranes are developed by blending alginate with CS and followed by crosslinking with MA. Fourier transform infrared (FTIR) spectral, X-ray diffraction (XRD), thermogravimetric analysis (TGA) and scanning electron microscope (SEM) were used to characterize the membranes and to understand the mechanism of interaction between the polymers constituting the blend and crosslinking agent. The pervaporative performance of the membranes in dehydrating EG was studied. The effect of experimental parameters such as feed composition, membrane thickness, and permeate pressure on separation performance of the crosslinked membranes was investigated.

2 Experimental

2.1 Materials

SA having an average molecular weight of 500,000 and CS having an average molecular weight of 300,000 were purchased from Aldrich Chemical Co., USA. Ethylene glycol, Excelar grade of purity 99.5%, was purchased from Qualigens Fine Chemicals, Mumbai. Isopropanol, maleic anhydride ($C_4H_2O_3$) and calcium chloride were purchased from Loba Chemicals, Mumbai. Water of conductivity <0.02 S/cm, used for the preparation of feed solutions, was generated in the laboratory by distilling the deionized water twice in a quartz distillation plant.

2.2 Membranes Preparation and Crosslinking

MA crosslinked CA/CS blend membranes were prepared via solution casting and solvent evaporation technique as discussed earlier (32). 2 wt% solutions of SA and CS were prepared separately by dissolving SA and CS in 2% oxalic acid. The suspensions were stirred for 2 h at 40–50°C. The solutions were allowed to stay overnight before used to enable the gas bubbles to escape. The casting solution was prepared by mixing together the SA and CS solutions in 1:3 ratio. The blend solution was then stirred for a period of 1/2 h for homogeneity and kept aside for 1 h to obtain a bubble free solution. The homogeneous solution was cast on to a clean glass plate and allowed to evaporate water to dryness at room temperature resulting in the formation of a dense non-porous blend membrane. The SA/CS blended membranes were pretreated with 2% $CaCl_2$ solution for 24 h at room temperature in order to improve its properties by replacing sodium ions by calcium ions (33). The resulting CA/CS membranes were washed with distilled water to remove excess calcium. CA/CS was further crosslinked with 3.5 wt% MA in a isopropanol-water (90/10 vol%) bath containing 1 vol% of concentrated H_2SO_4 as a catalyst. After crosslinking 3 h, the membranes were washed with water repeatedly and dried in an oven at 80°C and labeled as M-CA/CS. The average thickness of the each membrane was measured by a micrometer screw gauge.

2.3 Membrane Characterization

FTIR spectra of SA/CS and M-CA/CS membranes were scanned in the range between 4000 and 500 cm^{-1} using a Thermonicolet FTIR-200 series spectrophotometer.

A Seifert X-ray diffractometer was used to study the solid-state morphology of blended SA/CS and M-CA/CS in powdered form. X-rays of 1.546^{o}A radiation were generated by a CuK$_\alpha$ source at 40 kV and 20 mA. The angle of diffraction was varied from 5° to 60° to identify the changes in the crystal structure and intermolecular distances between the inter-segmental chains after crosslinking.

Thermal stability of the polymer films was examined using a Seiko 220TG/DTA analyzer, from 30 to 600°C at a heating rate of 10°C/min with continuous flushing with pure nitrogen gas at 200 ml/min. The samples were subjected to TGA to determine the thermal stability and decomposition characteristics.

The morphology of the SA/CS and M-CA/CS membranes were observed using Jeol SEM attached with x-ray energy analyzer model JSM-840A.

2.4 Sorption Studies

In order to evaluate membrane-liquid affinities, weighed samples of circular pieces of the polymer films (3 cm diameter) were soaked in EG/water mixtures of various concentrations. The swollen samples were taken out after different

soaking periods and quickly weighed after carefully wiping out excess liquid to estimate the amount absorbed at the particular time, t. The film was then quickly placed back in the solvent. The process was repeated until the films attained steady state as indicated by constant weight after a certain period of soaking time. Degree of swelling (DS) was calculated as,

$$DS = \frac{M_s}{M_d} \qquad (1)$$

The sorption represents the fraction of the extracted liquid mixture by the membrane. The percentage sorption was calculated using the equation:

$$\%Sorption = \frac{M_s - M_d}{M_d} * 100 \qquad (2)$$

Where M_s was mass of the swollen polymer in grams, and M_d was mass of the dry polymer in grams.

2.5 Determination of the Ion Exchange Capacity

The ion exchange capacity (IEC) indicates the number of milliequivalents of ions in 1 g of the dry polymer. The degree of substitution indicates the average number of acid groups present in the polymer. To determine the degree of substitution by acid groups, M-CA/CS and SA/CS specimens of similar weight were soaked in 50 ml of 0.01N NaOH solution for 12 h at ambient temperature. Then, 10 ml of the solution was titrated with 0.01N H_2SO_4. The membrane was regenerated with 1M HCl, washed with water until the washings are free from acid and dried to a constant weight. The IEC was calculated according to the equation,

$$IEC = \frac{(B - P) * 0.01 * 5}{m} \qquad (3)$$

Where B was the volume of H_2SO_4 used to neutralize blank sample soaked in NaOH (ml), P was the volume of H_2SO_4 used to neutralize the membrane soaked in NaOH (ml), 0.01 was the normality of the H_2SO_4, and "5" was the factor corresponding to the ratio of the amount of NaOH taken to dissolve the polymer to the amount used for titration, and m was the sample mass (g).

2.6 Pervaporation and Analytical Procedure

2.6.1. *Influence of operating conditions*

Experiments were carried out following the procedure described in the earlier literature (17, 32, 34). The indigenously constructed 100 ml batch level PV manifold (Figure 1) was operated at a vacuum as low as 0.5 mmHg in the permeate line. The effective area of the membrane in contact with the feed stream was 19.6 cm^2. The feed consisting of EG and water was stirred vigorously at a speed of 150 rpm during experiments to minimize concentration polarization. Permeate was condensed and collected in a liquid
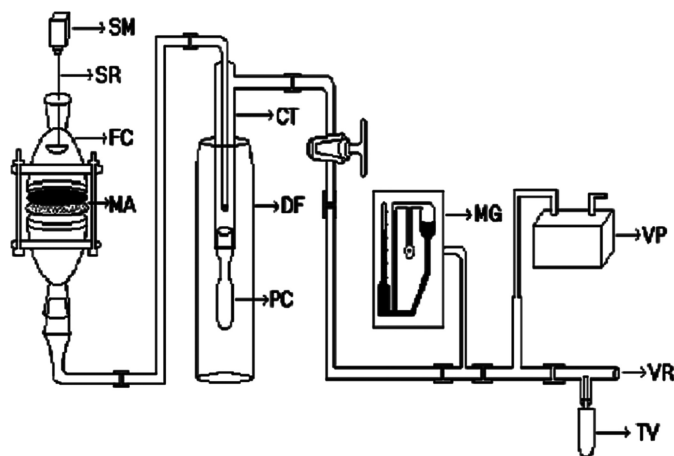
Fig. 1. Block diagram of pervaporation set-up. SM: stirring motor, SR: stirring rod, FC: feed chamber, MA: membrane assembly, CT: condenser trap, DF: Diwar flask, PC: permeate collector, MG: McLeod gauge, VP: vacuum pump, VR: vacuum release, TV: Teflon valve.

nitrogen cold trap for 6 h. Tests were carried out at room temperature (30 ± 2°C) and repeated twice using fresh feed solution to check for reproducibility. The collected permeate was weighed in a Sartorius electronic balance with an accuracy of 10^{-4} g to determine the flux. Analysis of permeate composition was carried out by measuring the refractive index of the mixture with an accuracy of ±0.001 units, using a Abbe Refractometer (Advance Research Instruments Company, New Delhi, India). A calibration plot of refractive index versus percent composition of water-EG was obtained with the known quantities of mixture components.

2.6.2. *Flux and selectivity*

The flux J of a given species, say faster permeating component i of a binary liquid mixture comprising of i(water) and j(EG) is given by:

$$J_i = \frac{W_i}{At} \qquad (4)$$

Where W_i represents the mass of water in permeate (kg), A is the membrane area (m^2) and t represents the experiment time (hr). PV flux on a commercial level is generally reported for a membrane of 10 μm thickness. The observed flux for a membrane of any given thickness is converted to flux for 10 μm by multiplication of the corresponding factor assuming linear relationship between thickness and flux.

The membrane selectivity (α) is the ratio of permeable coefficients of water and EG and can be calculated from their respective concentrations in feed (x) and permeate (y)
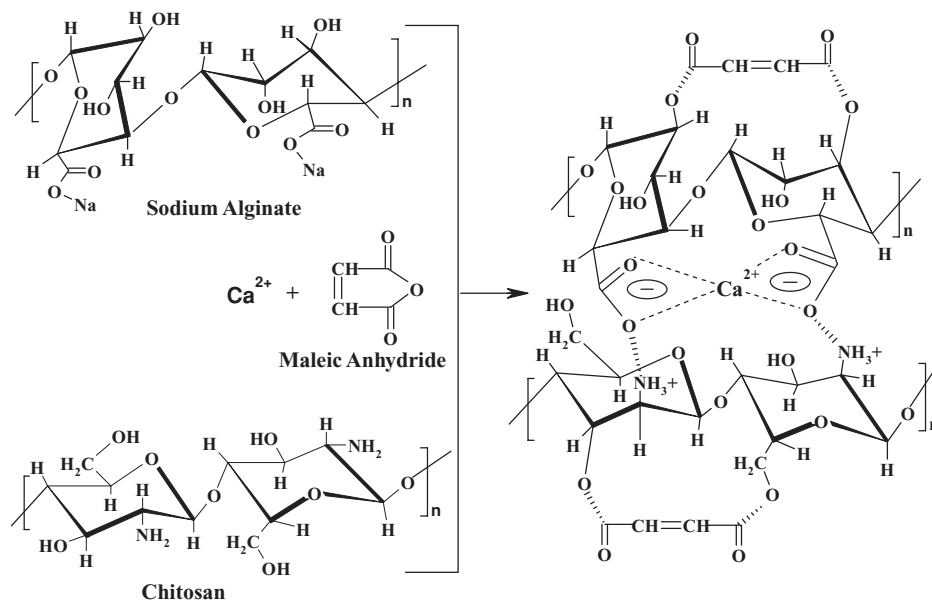
Sch. 1. Structural representation of sodium alginate/chitosan blended membrane pre-treated with calcium chloride and crosslinked with maleic anhydride.

as given below:

$$\alpha = \frac{y(1-x)}{x(1-y)} \qquad (5)$$

Pervaporation separation index (PSI), which is a measure of the separation capability of a membrane, is expressed as a product of selectivity (α) and flux (J),

$$PSI = J\alpha \qquad (6)$$

3 Results and Discussion

Alginate polymer contains D-mannuronic acid and L-guluronic acid. D-mannuronic acid exists in 1C conformation and is connected in the β-configuration through the 1- and 4- positions and L-guluronic acid has the 1C conformation and is α-1, 4- linked in the polymer (35). Because of the particular shapes of the monomers and their modes of linkage in the polymer, the geometries of the G-block regions, M-block regions, and alternating regions are substantially different. Specifically, the G-blocks are buckled while the M-blocks have a shape referred to as an extended ribbon. If two G-block regions are aligned side by side, a diamond shaped hole results. This hole has dimensions that are ideal for the cooperative binding of calcium ions. When calcium ions are added to a SA solution, such as alignment of the G-blocks occurs; the calcium ions are bound between the two chains like eggs in an egg box (36). Roger et al. (37) reported the complete conversion of SA in to CA occurs in about 10 min after addition of SA to calcium chloride solution. The SA/CS membrane was converted into CA/CS membrane on treatment with CaCl$_2$ and further crosslinked with maleic anhydride (MA).

A model of the possible interaction is shown in Scheme 1, which represents the formation of ionic complex between cationic group (–NH$_3^+$C) of chitosan polymer and anionic group (–COO$^-$) of alginate polymer (9). Further, the addition of MA induces covalent crosslinking and results in formation of H-bonding in addition to electrostatic interactions. It was noticed that the M-CA/CS blends were optically clear to the naked eye. No separation into two layers or any precipitation was noticed when allowed to stand for one month at room temperature. An estimation of the number of groups present before and after crosslinking gives an idea of the extent of crosslinking.

3.1 Membrane Characterization

3.1.1. *FTIR studies*
The FTIR spectrum of SA/CS (Figure 2(a)) shows the characteristic absorption band at 3610 cm^{-1} (broad signal of –OH and –NH-) and the broad band appearing at 1827 cm^{-1} confirms the presence of –NH$_3^+$C group in the SA/CS membrane. The other bands at 1671 cm^{-1} (amide), 1485 cm^{-1} (carboxylate), 1365 cm^{-1} (-CH$_2$ bending), 1202 cm^{-1} (-COO$^-$ group), 1183 cm^{-1} (C–C stretching) and 907 cm^{-1} (skeletal vibrations involving the C–O stretching) are the characteristics of SA/CS blend membrane structure (38). The spectrum confirms the complexation between the dissociated carboxylate groups of SA (COO$^-$) and protonated amino groups from CS through electrostatic interaction. Moreover, as the polyion complex
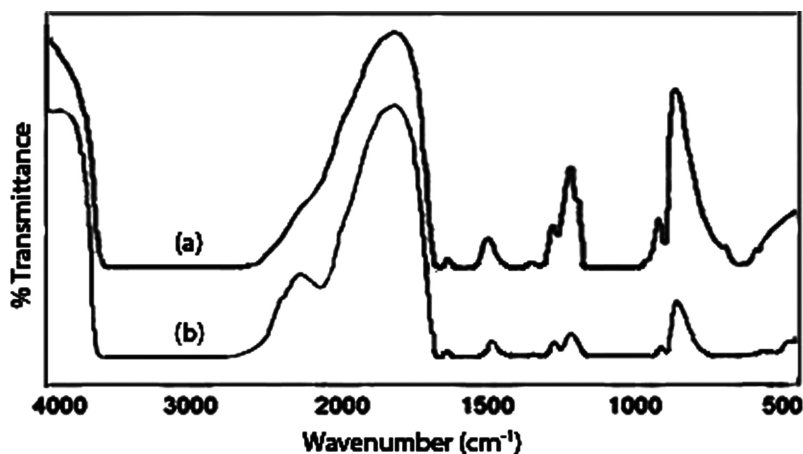
Fig. 2. FTIR spectra of (a) SA/CS and (b) M-CA/CS blend membranes.

formation proceeds, the O—H bonding would also be expected because of an increase in intermolecular interaction such as hydrogen bonding between SA and CS. In addition to the peaks observed in the spectrum of SA/CS membrane, the FTIR spectrum of M-CA/CS (Figure 2(b)) exhibits an absorbance band at 2215 cm^{-1}. This is the characteristic band of –CC(O)O–, indicating the presence of maleic anhydride in the membrane. The presence of calcium was confirmed by calcium elemental test. The model structure proposed in Scheme 1 was well in accordance with the FTIR spectra.

3.1.2. *XRD studies*

X-ray diffraction studies provide information on the nature of the compound, as well as on the spacing between the clusters of the polymer chains. On crosslinking, the polymer chains are in close compaction with one another and thus a reduction in the cluster space may be encountered. The effective *d*-spacing (*d*) gives an indication of cluster space existing in the polymer before and after crosslinking. The X-ray diffractograms of SA/CS and M-CA/CS blend membranes, shown in Figure 3, have no sharp peaks indicating the amorphous nature of the membranes. The XRD spectra of the SA/CS (Figure 3(a)) exhibits a broad peak at $2\theta = 20°$, which may be due to the intermolecular interaction such as the formation of hydrogen bonding between SA and CS (39). M-CA/CS membrane appears to be more amorphous than SA/CS as its diffraction pattern has no peak. On crosslinking the peak that appears at $2\theta = 20°$ in the diffraction pattern of SA/CS disappears due to disturbance of the bonds in M-CA/CS blended membrane. The *d*-spacing values are 4.3 A^o for SA/CS and 3.6 A° for M-CA/CS membranes. The reduction in effective *d*-spacing from 4.3 to 3.6 A° indicates the shrinkage in cell size or inter-segmental spacing occurring due to crosslinking, which would improve the selective permeation of the membrane.

3.1.3. *TGA studies*

The thermal degradation behavior of membranes was examined following the weight loss as function of temperature. The TGA curves for SA/CS and M-CA/CS are shown in Figure 4. The TGA curve of SA/CS blend exhibits a single weight loss stage ranging between 220–280°C followed by a final decomposition at 280°C. The weight loss stage can be attributed to the decomposition of main chain in the blend. The TGA curve of M-CA/CS blend exhibits two weight loss stages between 170–240°C and 260–350°C followed by a final decomposition around 450°C. The weight loss in the first stage can be attributed to decomposition of calcium chelate and covalent crosslinking of MA with SA and CS, and weight loss in the second stage can be attributed to splitting of the main chain before final decomposition of the polymer. TGA analysis indicates that the crosslinked (M-CA/CS) membrane possesses higher thermal stability than uncrosslinked membrane (SA/CS).

3.1.4. *SEM analysis*

The SEM micrograms of SA/CS and M-CA/CS were recorded to verify the compatibility between SA, CS and
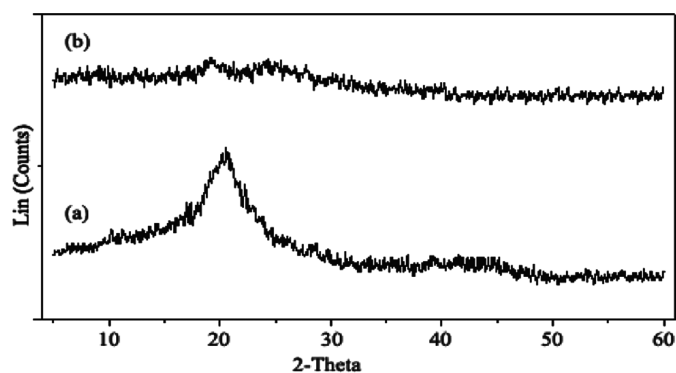

Fig. 3. X-ray diffractograms of (a) SA/CS and (b) M-CA/CS blend membranes.

Table 1. Effect of feed concentration on DS, % of sorption, normalized flux, selectivity and PSI values

Feed water (wt%)	Degree of swelling	% of sorption	Normalized flux (J). (kg.m^{-2}.h^{-1}.10 μm)	Selectivity (α)	PSI (J.α)
0.00	1.0319	3.1915	–	–	–
3.12	1.0651	6.5104	0.3843	302.4748	116.2411
8.10	1.1483	14.8337	0.4216	100.7657	42.4829
14.81	1.2459	24.5989	0.4685	42.6669	19.9937
20.11	1.3248	32.4873	0.5196	24.1822	12.5651
24.95	1.4278	42.7835	0.5751	11.9201	6.8553
100.00	2.7544	175.4385	–	–	–

MA molecules and to examine their surface morphology. The micrograms are shown in Figure 5. The micrograms of SA/CS and M-CA/CS show a smooth and homogeneous morphology indicating that the components used in the synthesis of the membranes are compatible with one another.

3.2 Sorption Phenomenon

The effect of equilibrium sorption percentage of M-CA/CS membrane in EG/water mixtures at different compositions is shown in Table 1. In pure water, the sorption was very high 175.43 and in pure EG it was 3.19. This shows the hydrophilic nature of the membrane, which has affinity for water and is capable of being selective towards the same during separation. The degree of swelling and sorption percentage correspondingly rises with an increase in the feed water concentration resulting in enhanced flux. However, increased swelling has a negative impact on membrane selectivity since the swollen and plasticized upstream membrane layer allows some EG molecules also to escape into the permeate side along with water.

3.3 Ion Exchange Capacity (IEC)

The amount of residual hydroxyl and acetyl groups in blend membranes after crosslinking was estimated from IEC studies. It was found that SA/CS blend had an IEC of 3.82 mequiv./g, whereas MA crosslinked polymer exhibited an IEC of 1.84 mequiv./g. The IEC results showed that almost 50% of hydroxyl groups present in the unmodified SA/CS have now formed crosslinks with MA. The IEC, which is equivalent to the total number of acetyl and hydroxyl groups present in the membrane, decreased upon crosslinking because some hydroxyl groups and acetyl groups were consumed during the reaction (32, 34). A model of the possible interaction shown in Scheme 1 represents the crosslinking reaction occurring between SA/CS blend, Ca^{2+} and MA. The membrane could withstand the solvent environment and PV conditions employed in this study.

3.4 Pervaporation Results

3.4.1. *Effect of feed composition*

PV experiments were performed over a wide range concentration of EG/water mixtures at 30°C to study the separation behavior of M-CA/CS membrane. In this study, the membrane thickness and permeate pressure were kept constant at 45 μm and 0.5 mmHg, respectively. Table 1 shows that an increase in the normalized flux from 0.38 to 0.57 kg.m^{-2}.h^{-1}.10 μm and decreased in selectivity from 302.4 to 11.9 as the feed water composition is increased
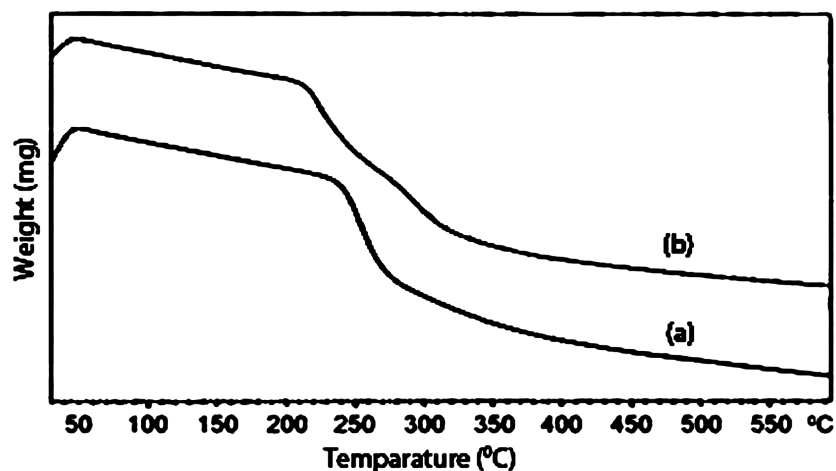
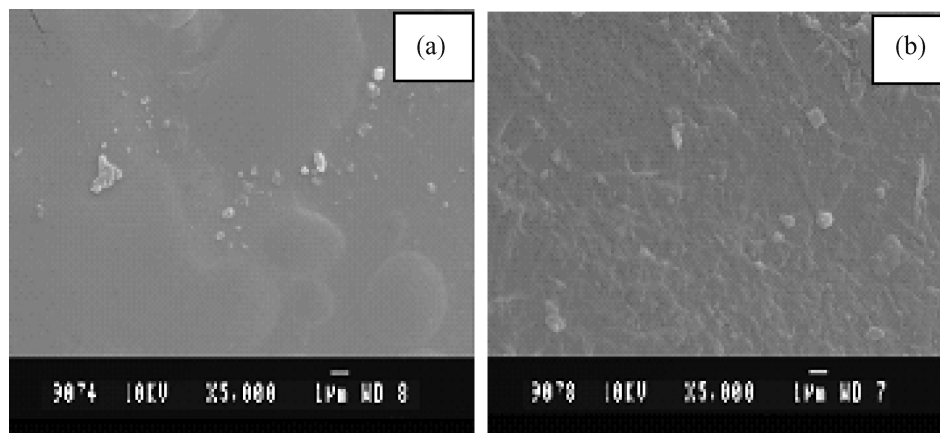**Fig. 4.** TGA curves of (a) SA/CS and (b) M-CA/CS blend membranes.

Fig. 5. SEM micrographs of (a) SA/CS and (b) M-CA/CS blend membranes.

from 3 to 25 wt% (Figure 6). Mass transport through the hydrophilic blend membrane occurs by solution diffusion mechanism (40). It was interesting to note that the total flux for the system increases substantially from 3 to 25 wt% water in the feed. This is due to the fact that the M-CA/CS membrane has a high affinity for water and is very hydrophilic in nature.

The separation performance of the membranes is evaluated in terms of the pervaporation separation index (PSI), which gives the combined result of selectivity and flux. The variation of PSI with the concentration of water in the feed is also shown in Table 1. From the Table, it is evident that the M-CA/CS membrane yields a higher value of PSI (116.2) at 3 wt% concentration of water in the feed, and it decreases with increasing feed water concentration. According to the PSI values, the M-CA/CS membrane performed a better separation at a higher feed EG concentration.

3.4.2. *Effect of membrane thickness*

The effect of varying membrane thickness on separation performance was studied at a constant feed composition of

92 wt% EG and permeate pressure at 0.5 mmHg by casting membranes of thickness ranging from 45 to 195 μm. Generally, selectivity was constant or increased marginally with rising thickness. With an increase in membrane thickness, a gradual reduction in flux from 0.094 to 0.071 kg.m^{-2}.h^{-1} is evident from Figure 7. Even though the availability of polar groups enhances with an increase in the thickness, flux decreases since diffusion of feed is retarded due to increased resistance to mass transfer. The permeate concentration of water varied from 89.88 to 95.56 wt%, which means that selectivity has increased from 100.7 to 245.5. In PV process, the upstream layer of the membrane was swollen and plasticized due to absorption of feed liquid and allowed unrestricted transport of feed components. In contrast, the downstream layer was virtually dry due to continuous evacuation (low pressure) in the permeate side, and therefore, this layer formed the restrictive barrier, thus allowing the interacting small size water molecules to pass through the membrane. It was expected that the thickness of the dry layer would increase with an increase in the overall membrane thickness
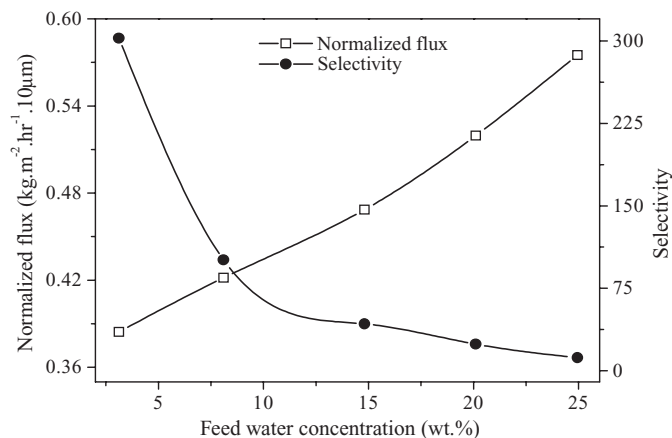

Fig. 6. Effect of feed water composition on PV performance of M-CA/CS membrane.
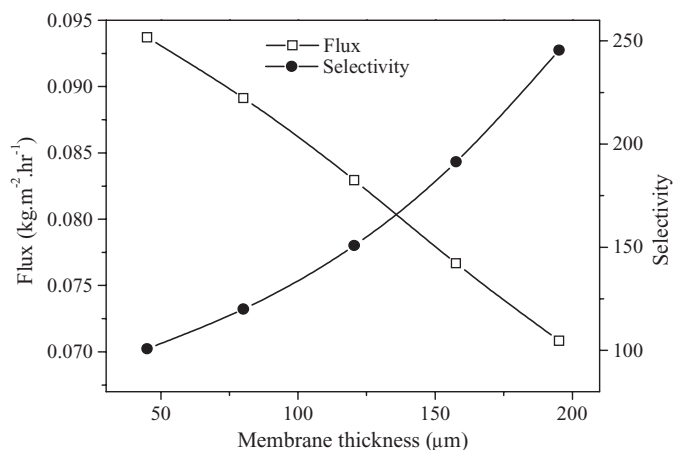

Fig. 7. Effect of membrane thickness on PV performance.

Table 2. Comparison of PV performance of M-CA/CS membrane with literature values

Membrane	Feed EG concentration (wt%)	Operating temperature (°C)	Flux (kg.m^{-2}.h^{-1})	Selectivity	Reference
CS/PAA	80	70	0.216	105	1
H$_2$SO$_4$-CS/PES	80	80	1.130	—	2
CS/PS	90	35	0.300	—	16
H$_3$PO$_4$-CS	96.4	30	0.378	234	17
Mordenite-CS/PAA	80	70	0.165	258	18
GA-PVA/PES	82.5	80	0.383	231	19
PVA/PS	85	80	0.680	—	20
GA-PVA/PES	80	70	0.427	438	21
PVA-Silica (basic)	80	70	0.067	311	22
PVA-Silica (acidic)	80	70	0.084	44	22
PVA (heat treatment)	80	70	0.145	54	23
PVA–GPTMS/TEOS	80	70	0.060	714	23
TMC-PVA/PS	90	60	0.360	987	24
GA-PVA	80	70	0.211	933	25
PAAM/PVA IPN	80	30	0.140	96	26
PAA/PVA IPN	80	30	0.480	196	26
SPE	90	80	0.454	44.5	27
GFT1510	90	75	1.700	—	28
SPEEK	80	70	0.067	1100	29
MA-CA/CS	96.8	30	0.085	302	Present work

PAA: poly acrylic acid, PES: Polyethersulfone, PS: polysulfone, GA: glutaraldehyde, GPTMS: γ-glycidyloxypropyltrimethoxysilane, TEOS: tetraethoxysilane, TMC: trimesoyl chloride, PAAM: polyacrylamide, SPE: sulfonated polyethylene, SPEEK: sulfonated poly(ether ether ketone).

resulting in improved selectivity as observed in the present study.

3.4.3. *Effect of permeate pressure*

The effect of permeate pressure on the crosslinked blend membrane was studied in the range of 0.5 to 9 mmHg at a constant membrane thickness of 45 μm and feed mixture containing 92 wt% EG. As the permeate pressure decreases, the driving force for diffusing molecules increases, resulting in high permeate rates. According to Figure 8 membrane exhibits a considerable lowering of normalized flux from 0.42 to 0.18 kg.m^{-2}.h^{-1}.10 μm. Similarly, selectivity

increased from 100.7 to 199.2. With the increasing permeate pressures, diffusion of the feed molecules through the membrane, which is the rate-determining step, becomes slow, whereas high vacuum exerts a larger driving force. Under lower vacuum conditions, the volatility of the feed components governs the separation selectivity of the membrane. EG, being less volatile than water, permeates slowly, thus increasing the selectivity.

PV performance of the M-CA/CS membrane is compared with the literature data and is reported in Table 2. From the Table, it can be noted that a marginally good selectivity and comparable fluxes render the crosslinked blend suitable for dehydration of EG/water mixtures. Furthermore, the ease in fabrication of these membranes associated with low cost render them more attractive for PV separation of aqueous EG mixtures.
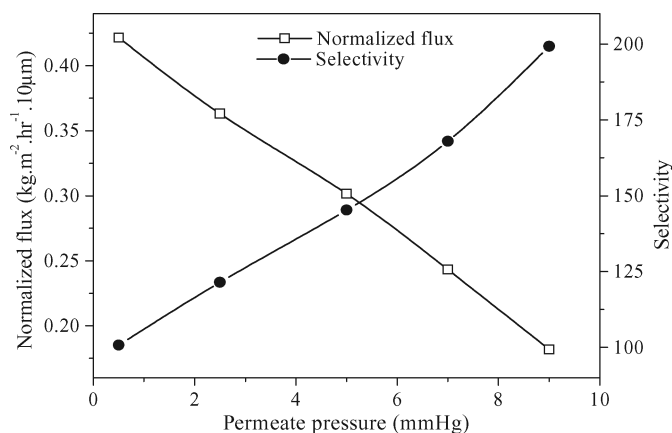
Fig. 8. Effect of permeate pressure on PV performance.

4 Conclusions

In the present study, the blend membrane of SA/CS was prepared, pre-treated with calcium chloride and further crosslinked with MA for PV based dehydration of EG/water mixture at 30°C. The number of groups crosslinked in SA/CS blend polymer was identified from the IEC studies. Characterization of the crosslinked membranes by FTIR and XRD confirmed the crosslinking reaction. The membranes showed adequate thermal stability to withstand the PV experimental conditions. FTIR

spectroscopy confirmed the predicted interaction between the SA/CS blend and the crosslinker. The permeate rate increases as the concentration of water in the feed increases; this mainly includes the contribution of both the increase of the degree of swelling, which enhances the expansion of the free volume, and the active effect of the diffusion coefficient of water through a membrane. In this case, pervaporation is proven as the most promising, alternative technology for the separation of aqueous-organic mixture of EG/water, particularly for the separation of close boiling mixtures.

Acknowledgements

References

1. Hu, C.L., Li, B., Guo, R.L., Wu, H. and Jiang, Z.Y. (2007) *Sep. Purif. Technol.*, 55(3), 327–334.
2. Nam, S.Y. and Lee, Y.M. (1999) *J. Membr. Sci.*, 153(2), 155–162.
3. Bravo, J.L., Fair, J.R., Humphrey, J.L., Martin, C.L., Seibert, A.F. and Joshi, S. *Fluid Mixture Separation Technologies for Cost Reduction and Process Improvement*; Noyes Data Corp.: Park Ridge, NJ, 1986.
4. Feng, X. and Huang, R.H.M. (1997) *Ind. Eng. Chem. Res.*, 36, 1048–1066.
5. Lipnizki, F., Field, R.W. and Ten, P.K. (1999) *J. Membr. Sci.*, 153(2), 183–210.
6. Wang, L.H., Li, J.D., Zhao, Z.P. and Chen, C.X. (2006) *J. Macromol. Sci. Part A: Pure Appl. Chem.*, 43, 305–314.
7. Satyanarayana, S.V. and Bhattacharya, P.K. (2004) *J. Membr. Sci.*, 238(1–2), 103–115.
8. Fang, J.H., Tanaka, K., Kita, H. and Okatomo, K.I. (2000) *J. Polym. Sci. Part A: Polym. Chem.*, 38(5), 895–906.
9. Kanti, P., Srigowri, K., Madhuri, J., Smitha, B. and Sridhar, S. (2004) *Sep. Purif. Technol.*, 40(3), 259–266.
10. Ye, H., Li, J., Lin, Y.Z., Chen, J. and Chen, C. (2008) *J. Macromol. Sci. Part A: Pure Appl. Chem.*, 45, 172–178.
11. Ye, H., Li, J., Lin, Y.Z., Chen, J. and Chen, C. (2008) *J. Macromol. Sci. Part A: Pure Appl. Chem.*, 45, 563–571.
12. Hara, M. (Ed.) *Polyelectrolytes: Science and Technology*; Marcel Dekker: New York, (Chapter 4), 1993.
13. Uragami, T. and Takigawa, K. (1990) *Polymer*, 31(4), 668–672.
14. Nawawi, M., Ghazali, M. and Huang, R.Y.M. (1997) *J. Membr. Sci.*, 124(1), 53–62.
15. Shieh, J.J. and Huang, R.Y.M. (1997) *J. Membr. Sci.*, 127(2), 185–202.
16. Feng, X. and Huang, R.Y.M. (1996) *J. Membr. Sci.*, 116(1), 67-76.
17. Rao, P.S., Sridhar, S., Wey, M.Y. and Krishnaiah, A. (2007) *Ind. Eng. Chem. Res.*, 46, 2155–2163.
18. Hu, C.L., Guo, R.L., Li, B., Ma, X.C., Wu, H. and Jiang, Z.Y. (2007) *J. Membr. Sci.*, 293(1–2), 142–150.
19. Chen, F.R. and Chen, H.F. (1996) *J. Membr. Sci.*, 109(2), 247–256.
20. Bartels, C.B. and Reale, J. (1989) US Patent 4, 802, 988.
21. Guo, R.L., Fang, X., Wu, H. and Jiang, Z.Y. (2008) *J. Membr. Sci.*, 322(1), 32–38.
22. Guo, R.L., Ma, X.C., Hu, C.L. and Jiang, Z.Y. (2007) *Polymer*, 48(10), 2939–2945.
23. Guo, R., Hu, C., Pan, F., Wu, H. and Jiang, Z. (2006) *J. Membr. Sci.*, 281(1–2), 454–462.
24. Hyder, M.N., Huang, R.Y.M. and Chen, P. (2008) *J. Membr. Sci.*, in press.
25. Guo, R., Hu, C., Li, B. and Jiang, Z. (2007) *J. Membr. Sci.*, 289(1-2), 191–198.
26. Burshe, M.C., Sawant, S.B., Joshi, J.B. and Pangakar, V.G. (1998) *Sep. Purif. Technol.*, 13(1), 47–56.
27. Pasternak, M. and Real, J. (1993) US Patent 5, 182, 022.
28. Jehle, W., Staneff, T., Wagner, B. and Steinwandel, J. (1995) *J. Membr. Sci.*, 102, 9–19.
29. Huang, R.Y.M., Shao, P., Feng, X. and Anderson, W.A. (2002) *Ind. Eng. Chem. Res.*, 41, 2957–2965.
30. Shao, P., Huang, R.Y.M., Feng, X., Anderson, W., Pal, R. and Burns, C.M. (2005) *J. Membr. Sci.*, 254(1–2), 1–11.
31. Du, J.R., Chakma, A. and Feng, X. (2008) *Sep. Purif. Technol.*, 64(1), 63–70.
32. Reddy, A.S., Kalyani, S., Kumar, N.S., Boddu, V.M. and Krishnaiah, A. (2008) *Polym. Bull.*, 61, 779–790.
33. Yang, G., Zhang, L., Peng, T. and Zhong, W. (2000) *J. Membr. Sci.*, 175(1), 53–60.
34. Kalyani, S., Smitha, B., Sridhar, S. and Krishnaiah, A. (2006) *Ind. Eng. Chem. Res.*, 45, 9088–9095.
35. Badwan, A.A., Abumalooh, A., Sallam, E., Abukalaf, A. and Jawan, O. (1985) *Drug Dev. Ind. Pharm.*, 11, 239–256.
36. Rendevski, S.J. and Andonovski, A.N. (2005) *Polym. Bull.*, 54, 93–100.
37. Roger, S., Talbot, D. and Bee, A. (2006) *J. Magnet. Magnet. Mater.*, 305(1), 221–227.
38. Yin, Y.J., Yao, K.D., Cheng, G.X. and Ma, J.B. (1999) *Polym. Int.*, 48, 429–432.
39. Kim, J.H. and Lee, Y.M. (1993) *Polymer*, 34(9), 1952–1957.
40. Osada, Y. and Nakagawa, T. (Eds.) *Membrane Science and Technology*. Marcel Dekker Inc.: New York, 1992.